Z. Phys. Chem. **217** (2003) 299–313
© by Oldenbourg Wissenschaftsverlag, München

Electrochemical Micromachining of Stainless Steel by Ultrashort Voltage Pulses

By Laurent Cagnon[1], Viola Kirchner[1], Matthias Kock[1], Rolf Schuster[1,*], Gerhard Ertl[1], W. Thomas Gmelin[2], and Heinz Kück[2]

[1] Fritz-Haber-Institut der Max-Planck-Gesellschaft, 14195 Berlin, Germany
[2] IZFM, Universität Stuttgart, 70174 Stuttgart, Germany

Dedicated to Prof. Dr. Dieter M. Kolb on the occasion of his 60th birthday

(Received and accepted July 15, 2002)

Stainless Steel / Microstructures / Microfabrication / Electrochemistry / Short Voltage Pulses

Application of ultrashort voltage pulses to a tiny tool electrode under suitable electrochemical conditions enables precise three-dimensional machining of stainless steel. In order to reach submicrometer precision and high processing speed, the formation of a passive layer on the workpiece surface during the machining process has to be prevented by proper choice of the electrolyte. Mixtures of concentrated hydrofluoric and hydrochloric acid are well suited in this respect and allow the automated machining of complicated three-dimensional microelements. The dependence of the machining precision on pulse duration and pulse amplitude was investigated in detail.

1. Introduction

The progress of modern electronics technology towards smaller devices triggered the miniaturization of mechanical and optical parts and components like sensors, connectors, actuators or reactors [1–6]. Besides semiconductors, metals become increasingly important to fulfill the specifications of such applications. Molding techniques for the mass production of plastic microcomponents [7] require the fabrication of molds from hard materials, preferentially alloyed steels. However, methods which allow for the three-dimensional micromachining of metals are rather limited. Although conventional mechanical methods like milling or electrical discharge machining were steadily improved,

* Corresponding author: E-mail: schuster@fhi-berlin.mpg.de

in the lower micrometer to nanometer range only very restricted techniques are available [8]. Particularly electrochemical techniques became valuable tools for the fabrication of microelements, which benefit from the absence of mechanical or thermal stress, induced by most machining methods like milling or laser ablation. For example the LIGA process belongs into this category where by a combination of lithographic techniques and electrochemical metal deposition small, essentially two-dimensional structures can be produced [9]. Also partial isolation of the electrodes by patterned masks is employed [10, 11], *e.g.*, for the etching of small nozzles for ink jet printers.

The various electrochemical microstructuring methods can be separated into two groups. In the 'top down' approach the electrochemical reactions are localized on the workpiece surface by employing geometrical constraints. Macroscopic amounts of material are removed in parallel and the shape of the tool electrode or the pattern of a mask is directly imprinted onto the workpiece. On the other hand, in the 'bottom up' approach small amounts of material are sequentially manipulated and the desired structure is built up from small entities like clusters consisting of only a few atoms. The combination of electrochemical techniques with scanning probe microscopy provides a fascinating tool on such atomic scale. The most prominent electrochemical method in this respect certainly is the local, mechanical deposition of small metal clusters of only a few hundred atoms with a tiny STM tip, where the metal was previously electrochemically deposited, developed in Kolb's group at the University of Ulm. The precise deposition of arrays of thousands of clusters was impressively demonstrated [12, 13]. Other methods include local deposition of small Co clusters by electrochemical redissolution from an STM tip [14] and the local Ag, Pt or Cu cluster deposition on graphite [15, 16] or Au surfaces [17, 18] by local nucleation in small holes, previously formed by voltage pulses to an STM tip. Similarly, atomic steps on a single crystalline surface were used as nucleation sites for the electrochemical deposition of metallic nanowires [19].

Although these 'bottom up' methods allow for the precise manipulation on almost atomic scale, their use for the machining of complicated three dimensional structures on the micrometer scale seems rather restricted, as long as they suffer from slow machining speed and specialized materials. On the other hand most electrochemical 'top down' methods have to circumvent the problem of weak spatial resolution of conventional electrochemistry: Upon polarization of electrodes immersed into an electrolyte the applied potential drops mainly in the electrochemical double layers on the electrode's surfaces, which reach only a few water layers deep into solution. Since the rates of the electrochemical reactions are governed by the potential drop in the double layer (DL), the shape and position of the counter electrode are only of secondary influence on the reactions on the electrodes' surfaces.

An often-applied solution to locally influence the reaction rates at a workpiece is to manipulate the density of the Faradaic current, passing through

the electrolyte. This is performed in two ways, either by local insulation of one or both of the electrodes [20, 21] or by making use of the ohmic potential drop in the electrolyte due to high Faradaic currents at high overpotentials. Both methods exist in various sophisticated modifications. Recently the spatial resolution of conventional electrochemical countersinking, where DC voltages of up to 40 V are applied to the electrodes, has been improved down to the 10 μm range by reducing the gap width between the negatively shaped tool electrode and the workpiece. To supply fresh electrolyte and to remove dissolved material from the gap, it is cyclically opened, after switching off the cell voltage [22]. Small holes with diameters down to about 10 μm, *e.g.*, in turbine blades or injection nozzles, were electrochemically drilled with small electrolyte-filled glass capillaries, where the electrochemical reactions are confined close to the orifice of the capillary [23]. Even higher spatial resolution, although restricted to the fabrication of shallow indents, was achieved with the help of ultramicroelectrodes in the scanning electrochemical microscope [24–26]. Holes in thin metal films were produced by through mask etching, and the inverse process, the electrochemical deposition, *e.g.*, of Cu and Ni into patterned masks is employed in the LIGA process for the mass production of metallic microelements with precisions better than 100 nm and a thickness up to several hundred micrometers. However, although obtaining highest precision, close to that obtained with 'bottom up' techniques, all mask techniques allow basically only for the fabrication of two-dimensional structures. Inclined walls or three-dimensional structures are difficult, if not even impossible, to be fabricated with these methods.

Recently we introduced a different approach, where electrochemical reactions are spatially confined with down to nanometer precision through the application of ultrashort voltage pulses [27, 28]. This technique may help to bridge the gap between the versatility of the 'top down' and the precision of the 'bottom up' methods for three dimensional electrochemical microstructures. With this method, the electrochemical reaction rates on the workpiece surface are directly controlled by local polarization of the double layer. It employs the finite time constant for the polarization of the double layer (DL) upon a voltage pulse. This time constant is given by the product of the electrolyte resistance along the current path and the double layer capacitance, and therefore varies linearly with the separation between the electrodes. By application of ultrashort voltage pulses between a workpiece and a tiny tool electrode, the DL at the workpiece is only noticeably charged, where both electrodes are in close proximity, *i.e.*, where the electrolyte resistance along the current path is low enough to allow significant flow of charging current. Since the rate of electrochemical reactions is exponentially dependent on the voltage drop in the DL, the reaction at the workpiece is strongly confined to the charged region. As described in detail in Ref. [27] and Section 4, assuming typical DL capacitance and specific electrolyte resistance, pulses of a couple of 10 ns duration confine the charging of the DL to areas on the electrode surfaces, where the distance between

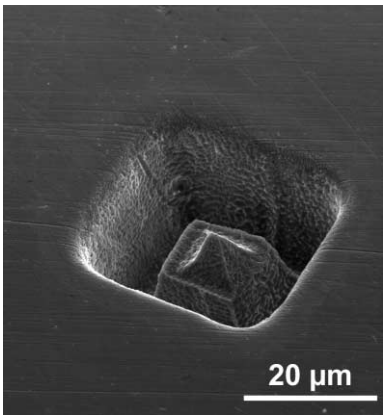

Fig. 1. Pyramid, etched into a stainless steel sheet with the electrochemical pulse method. A conically shaped W wire with less than 5 µm diameter was moved similar to a miniature milling cutter. Etched with 25 ns/2 V pulses in 3 M HCl/6 M HF ($\Phi_{wp} = -200\,mV_{Pd/H}$, $\Phi_{tool} = -100\,mV_{Pd/H}$).

the tool and the workpiece electrode amounts to less than a few micrometers. We achieved a machining precision of about 200 nm for the etching of stainless steel by 5 ns pulses as discussed later.

During etching with short voltage pulses the tool electrode can be molded precisely into the workpiece. Additionally, by moving the tool in three dimensions similar to a miniature milling cutter, individual three-dimensional microstructures can be machined from any electrochemically active material. The method has been successfully demonstrated for the micromachining of metals, alloys and semiconductors. In this paper we present results on the machining of stainless steel. The mechanical strength and chemical resistance of stainless steel can be widely varied by adjusting the alloy composition. Therefore, stainless steel is one of the most widely used construction material for applications ranging from chemical plants to chirurgical microtools. Its resistance against corrosion imposes special requirements on the composition of the electrolyte to prevent passivation of the workpiece during the electrochemical machining process. In detail the etching of the highly alloyed austenitic 1.4301 steel in acidic and highly concentrated halogenide electrolytes will be presented. It is demonstrated how machining rate, spatial resolution and surface quality can be controlled.

Fig. 1 shows a small pyramid, machined directly into a stainless steel sheet with a thin conical tungsten tip, whose tip angle defined the slope of the pyramid's faces. The structure of the pyramid is well defined on micrometer scale with sharp edges with radii of curvature smaller than 1 µm. The etched faces show a roughness in the submicrometer range, whereas the surface around the structure still exhibits the original morphology of the sheet with the scratches

from polishing still visible. This indicates the strong localization of the electrochemical reactions due to the exponential decay of the etching rate with increasing distance.

The pyramid was laid open by etching a stainless steel sheet in 3 M HCl/6 M HF electrolyte by 25 ns short voltage pulses (2 V amplitude, average potential of the workpiece $\Phi_{wp} = -200\,mV_{Pd/H}$, and tool $\Phi_{tool} = -100\,mV_{Pd/H}$). Concentrated acidic, halogenide-ions containing solutions are very well suited to overcome the passivation of the stainless steel surface against corrosion and to allow for successful electrochemical machining. The proper choice of the electrolyte's composition and the determination of the average potentials of the electrodes are discussed in detail in Section 3. In Section 4 the influence of the machining parameters like pulse duration and amplitude on the spatial resolution is investigated and compared with theoretical predictions. Experimental details are described in Section 2.

2. Experimental

The experimental setup comprises the control of the potentials of workpiece and tool, the electronics for providing the nanosecond voltage pulses, and features for the three dimensional manipulation of the tool electrode. The workpiece was immersed in an electrochemical cell mounted on a piezo-driven *x*-*y*-*z* stage, which was equipped with strain gauges (Tritor 3D 100 NV, Piezosystem Jena) and allowed the control of the absolute position of the workpiece with respect to the tool electrode with an accuracy better than 0.1 μm.

As samples we used 0.1 mm thin sheets of austenitic 1.4301 stainless steel which contains 18% Cr and 9% Ni. They were mechanically ground and polished with diamond paste down to 3 μm grain size. The tool electrodes were prepared from thin wires of either Pt or W. Cylindrically shaped tools were fabricated from Platinum wire, 50 μm in diameter, whose front face was mechanically ground and polished with Si-C and Al_2O_3 paper. During polishing the wire was embedded into a dissolvable resin for stability. Thinner and mechanically more stable tool electrodes were electrochemically etched from tungsten wires in 2 M KOH with a loop of a gold wire serving as counter electrode, similar to the fabrication of STM tips [29]. To reduce electrochemical currents during the machining experiments, the upper shafts of the tools were electrically insolated with a thermoplastic wax (Apiezon W).

The average potential of workpiece (Φ_{wp}) and tool electrode (Φ_{tool}) were controlled separately by a bipotentiostat [30]. Low-pass filters at its inputs suppress the high frequency components. The potentials were adjusted by a Pt counter electrode (CE) versus a palladium wire saturated with hydrogen (Pd/H), which served as reference electrode (RE). The wire was prepared prior to the machining experiment by electrochemical hydrogen evolution in diluted sulfuric acid for at least 20 minutes.

Trains of rectangular voltage pulses with a pulse to pause ratio of 1:10 generated by a high frequency pulse generator were applied between tool and workpiece. To match the impedance of the high frequency cables with that of the electrochemical cell, a high-speed buffer amplifier was mounted close to the tool electrode. The high frequency cell current and the pulse shape at the tool electrode were monitored with a real-time oscilloscope. Amplitude and shape of the cell current transient reflect directly the charging behavior of the double layer, *i.e.*, the actual distance between tool and workpiece [27], and were used to in-situ check the machining process.

The motion of the tool during the machining process was computer controlled. Occurrence of electric shortcuts between tool and workpiece electrodes, signaling too high feeding rates, was used to adjust the feeding rate of the tool. Immediately after a contact was detected the wire was retracted along the milling path until the contact was released. Subsequently the tool was fed again in the forward direction. Additionally, this back- and forward movement flushes the electrolyte and enforces the removal of dissolved material from the narrow gap between the two electrodes. The maximum feeding rate achieved in our experiments is dependent on the machining parameters. For the conditions of Fig. 1, lateral feeding rates of about 1 μm/s were achieved.

3. Electrochemical conditions for stainless steel micromachining

Prerequisite for the electrochemical micromachining with ultrashort voltage pulses is fast and homogeneous electrochemical dissolution of the workpiece in direct vicinity of the tool electrode. However, it is just the characteristic of stainless steel that it is resistant against corrosion even upon application of moderate potentials, where its constituents should be dissolved from the thermodynamic point of view [31]. In this so-called passive region practically no electrochemical current is flowing, due to the formation of a passive layer. Metal atoms of the alloy are oxidized to hydroxides and oxides and form an only few nanometers thick, but dense film on the surface. High Cr and Ni contents in the alloy stabilize this film, which inhibits further oxidation and dissolution of the material. Only at very positive potentials, in the so-called transpassive region, ion transport in the passive layer sets in and the steel is anodically dissolved accompanied by oxygen evolution. For 1.4301 stainless steel in 3 M HCl/6 M HF electrolyte, the passivation peak can be found at around $+0.2\,V_{Pd/H}$ and the passive region extends to about $+1.5\,V_{Pd/H}$.

Halogenide ions are known to chemically destabilize the passive layer. In the presence of Cl^- ions the dissolution of most stainless steels starts already in the passive region by the local formation of etch pits [32], one of the major reasons for corrosion problems caused by sea water or in chemical plants. On the other hand, technical processes exploit the weakening of the passive layer by halogenides. *E.g.*, in conventional electrochemical machining highly

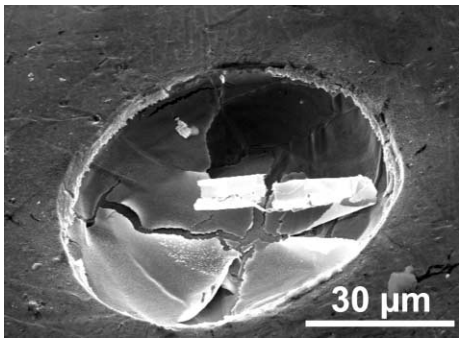

Fig. 2. Oxide flitters peeling off the surface of a hole machined in 1 M HCl with 500 ns/2 V pulses.

concentrated NaCl electrolytes are used for fast dissolution of stainless steel. Typically, the process is conducted in the transpassive region and voltages of 10 to 40 V (DC or low frequency AC) are applied between tool and workpiece [33].

It seems to be straightforward to use Cl^- containing electrolytes also for the electrochemical micromachining with ultrashort voltage pulses. Therefore, in first experiments we used 1 M HCl as electrolyte. The average potential of the workpiece was adjusted to the so-called active region of the surface, where the passive layer is not yet formed. However, upon application of pulses with up to 3 V amplitude and pulse durations between 50 ns and 500 ns the etching usually stopped after penetrating a few micrometers into the surface. Although no electrical contact could be detected, further feed of the tool was impossible without mechanical deformation. Inspection of the etched holes typically showed the formation of a film, which eventually peels off the surface (Fig. 2). We interpret these as flitters of a thick oxide film, which were electrochemically formed at the steel surface and which grew mechanically unstable due to their increasing thickness with progressing oxidation. These loose oxide flitters effectively insulate the workpiece surface and the electrochemical machining stops. In conventional electrochemical machining, where the distance between the electrodes is rather in the 100 µm to mm range, they are just underetched and form the so-called anode mud, which is usually rinsed away by agitation of the electrolyte. However, in electrochemical micromachining the size of these oxide flitters exceeds the gap width between the electrodes and therefore hinders the etching. Machining with high pulse voltages up to 20 V, *i.e.*, working in the transpassive region of the stainless steel dissolution, did not reliably solve the problem. In addition, the tiny tool electrodes often were destroyed by such high voltages.

It turned out that the formation of a thick oxide layer could be chemically prevented by employing more ‘aggressive’ electrolytes. With an aqueous so-

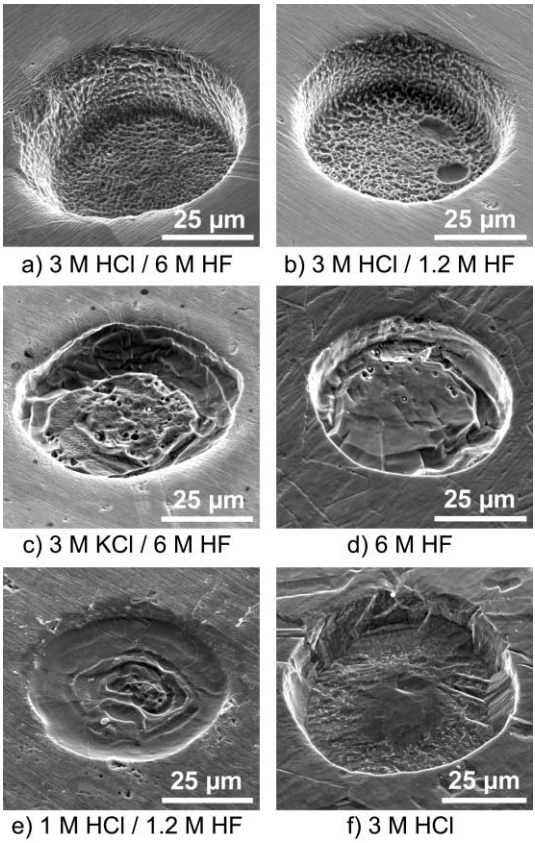

Fig. 3. Comparison of holes drilled into stainless steel in different electrolytes (Tool: cylindrical Pt wire of 50 µm diameter; pulses: 50 ns/2 V; $\Phi_{wp} \approx -100\,mV_{Pd/H}$, $\Phi_{tool} \approx 100\,mV_{Pd/H}$).

lution of 3 M HCl and 6 M HF we found an electrolyte mixture which allows the precise electrochemical etching and very fast micromachining of 1.4301 stainless steel (Fig. 1, Fig. 3a). Pulse amplitudes of only 1.5 to 2 V allowed machining rates up to several micrometers per second. On the other hand, by proper adjustment of the average surface potential to about $-200\,mV_{Pd/H}$, significant overall corrosion of the surface could be avoided for several hours.

In order to check the influence of the different ions in the mixture of hydrochloric and hydrofluoric acid we performed several experiments with different electrolytes (Fig. 3). A flattened, cylindrical 50 µm Pt-wire served as tool electrode in these experiments and was etched into the surface with 50 ns, 2 V pulses. High acidity of the electrolyte seems to be an important precondition for successful micromachining. Upon increasing the pH to about pH 3

and leaving the halogenide ion content constant by substituting HCl by KCl (3 M KCl/6 M HF), the etching almost ceased and the feeding rate of the tool became very low. The etched structures exhibited a porous bottom, which might be indicative of pit formation due to the high Cl^- content (Fig. 3c). Indeed, in pure 6 M HF (Fig. 3d) the etching produced rather smooth surfaces, although proceeding very slowly. The necessary fluoride content is strongly dependent on the HCl concentration. In 3 M HCl electrolytes the HF concentration could be reduced from 6 M to 1.2 M without degrading the machining process (Fig. 3b). However, in 1 M HCl/1.2 M HF micromachining was almost impossible (Fig. 3e). In pure 3 M HCl (Fig. 3f) etching proceeds very slowly and irreproducibly. However, increasing the HCl concentration to about 5 M enables the machining even in the absence of fluoride. In halogenide free acids such as sulfuric acid the electrochemical micromachining of stainless steel did not succeed. We conclude that the presence of high concentrations of halogenide ions together with a low pH chemically prevents the formation of thick oxide films on the stainless steel surface under our machining conditions.

It should be mentioned at this point that also the presence of complexing agents might prevent the formation of thick oxide layers. First experiments in saturated KCl electrolyte with 2.7 M citric acid showed promising results. By application of 1.5 to 4 V pulses (100 to 200 ns) 10 μm deep holes could be etched within about 5 minutes. The machining rate was more than an order of magnitude slower than for 3 M HCl/6 M HF and the process was rather sensitive towards accidental shortcuts between the electrodes upon which the surface became irreversibly passivated. Further studies on such less toxic and aggressive electrolytes are in progress.

In addition to the chemical composition of the electrolyte, the electrochemical parameters like the average potentials of workpiece and tool electrodes and the pulse amplitude are of equal importance for successful machining. The overall corrosion of both, workpiece and tool has to be avoided, which would favor potentials as negative as possible. However, too strong hydrogen evolution at tool or workpiece displaces the electrolyte from the electrode surfaces and therefore hinders the electrochemical machining. On the other hand, it turned out that moderate hydrogen evolution, which takes place at the tool electrode as local counter reaction to the local dissolution of the workpiece, effectively agitates the electrolyte and helps to remove debris from the machining region. For the electrolyte mostly used in this study for the machining of stainless steel, 3 M HCl/6 M HF, the workpiece surface was stable for several hours without significant corrosion at average potentials near $-200\,mV_{Pd/H}$. At this potential the surface is not covered by a passive layer, which turned out to be a prerequisite for the machining of stainless steel in HCl/HF electrolytes. If the average potential of the workpiece is held in the passive region, no etching with short pulses is possible, not even if the pulses polarize the surface into the transpassive region. Probably, ion transport through the passive layer is occurring on a time scale much longer than the pulse duration.

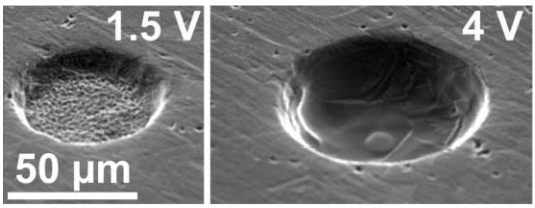

Fig. 4. Holes drilled into stainless steel with different pulse amplitudes employing the same cylindrical tool (50 µm diameter). 1.5 V pulses yielded sharp structures with micro porous surfaces. With 4 V pulse amplitude electropolished surfaces were achieved (Pulse duration: 50 ns; 3 M HCl/6 M HF; $\Phi_{wp} = -120\,mV_{Pd/H}$, $\Phi_{tool} = 80\,mV_{Pd/H}$).

Starting from the active potential region the applied pulse amplitude had to exceed about 1.5 V to dissolve the steel properly. Because the double layers of both, tool and workpiece are charged upon application of a voltage pulse, the pulse amplitude is shared between these two capacitances. Therefore, the polarization of the workpiece double layer during a pulse amounts roughly to about half the pulse amplitude. A typical pulse amplitude of 1.5 V, starting from an average potential of about $-200\,mV_{Pd/H}$, will achieve a local polarization of the workpiece corresponding to potentials in the passive region. However, due to the short pulse duration of only nanoseconds no dense passive layer is formed, since otherwise we could not machine the surface. This demonstrates that data obtained with conventional cyclic voltammetry with scan rates of typically 50 mV/s cannot directly be transferred to processes on nanosecond timescale. The absence of passivation in our experiment is conceivable, considering that even at the highest machining rates the material removal per pulse amounts only to about one hundreds of a monolayer. In contrast the thickness of the passive layer amounts to several nanometers [31].

The pulse amplitude also influences the surface quality (Fig. 4). Whereas with 1.5 V pulses the surface of the machined hole exhibits roughness on submicrometer scale, for 4 V pulses the machined surface appears smooth and the grain structure of the stainless steel sheet becomes visible. This is similar to DC machining of stainless steel, where the application of higher cell voltages also leads to electropolishing of the surface.

4. Spatial resolution

The method exploits a general characteristic of electrochemical systems. As mentioned above electrochemical reactions are governed by the potential drop in the electrochemical double layer at the interface of an electrode with the electrolyte. This double layer (DL), consisting of ions in front of the electrode and the corresponding influenced charge of opposite sign on the electrode's surface constitutes a plate capacitor with a specific capacitance c_{DL}. Upon

application of a voltage step between two electrodes the double layer capacitances are charged by a capacitive current flowing through the electrolyte with a finite specific resistance ρ. Therefore, the voltage drop in the DL follows an exponential time law with a charging time constant τ, given by the product of double layer capacitance C and local electrolyte resistance R along the current path. For a one-dimensional case the latter is proportional to the local distance d between the electrodes and the specific electrolyte resistance ρ: $\tau = RC = \rho\, c_{\mathrm{DL}} d$. Here the idea of ultrashort voltage pulses comes into play. Switching the voltage off after a short time t allows for significant charging of the DL only, where the local time constant τ becomes shorter or equal to t. Since electrochemical reaction rates are in general exponentially dependent on the polarization of the DL, reactions like the dissolution of the workpiece are strongly confined to electrode areas, where the DL is significantly charged, *i.e.*, where the electrodes are in very close proximity.

The above formula readily implies that the shorter the pulses are, the smaller the separation of the electrodes has to be for significant charging of the DL. In particular the distance between the electrodes up to which the electrochemical reactions take place with a significant rate of removal of material, which is equivalent to the spatial resolution of the method, is expected to vary linearly with the pulse duration. This has been previously demonstrated for the machining of Cu [27] and is shown in the following within a slightly different experiment for the machining of stainless steel. For this purpose a cylindrical tool electrode was positioned 0.5 μm in front of the stainless steel surface. In subsequent experiments pulses with durations between 7 ns and 200 ns and pulse to pause ratios of 1:10 were applied for 5 min. The width of the gap between the face of the tool and the bottom of the resulting holes is plotted in Fig. 5 versus the pulse duration. Particularly for small pulse durations, the gap width, *i.e.* the spatial resolution, scales linearly, as indicated by the line. For longer pulse durations probably mass transport limitations lower the rate of material removal and therefore the achieved depth of the hole.

The above relation for the time constant provides a rough estimate for the spatial resolution of the method, since the local distance d between the electrodes can be considered as measure for the spatial resolution. The local time constant for double layer charging, determined by the local distance of the electrodes d, should amount to less or equal the pulse duration. To match the experimental conditions we assume an specific electrolyte resistance of 2 Ω cm and a typical DL capacitance of 10 μF/cm^2. Solving the equation for d for a pulse duration of 50 ns leads to an expected resolution of about 25 μm. This is significantly larger than the observed spatial resolution for the same pulse duration in Fig. 5. However, the above approximation completely disregards the absolute amount of the electrochemical reaction rate, which together with the machining time determines the amount of dissolved material during the experiment. A crucial experimental parameter in this respect is the pulse amplitude which determines the maximum achievable machining rate. This is demon-

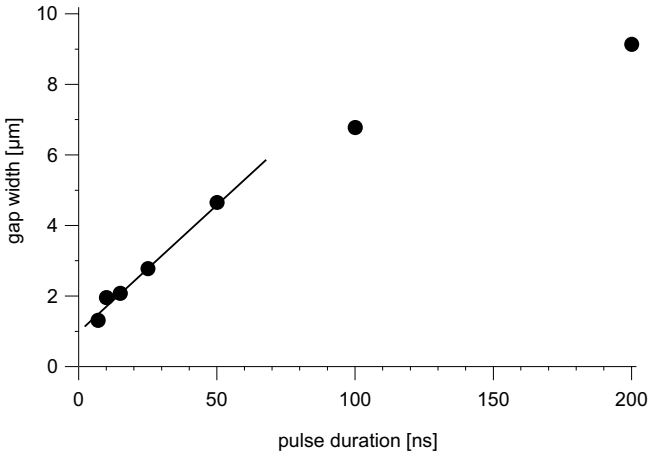

Fig. 5. Spatial resolution versus pulse duration. The gap width under the face of a 50 µm diameter cylindrical tool was determined for different pulse durations. The tool was positioned 0.5 µm above the stainless steel surface and pulses with 1.6 V amplitude were applied for 5 minutes (3 M HCl/6 M HF; $\Phi_{wp} = -270\,mV_{Pd/H}$, $\Phi_{tool} = -370\,mV_{Pd/H}$).

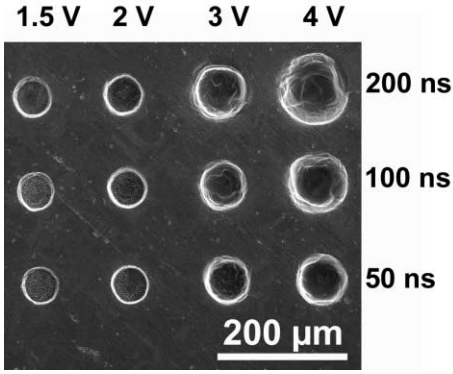

Fig. 6. Array of holes drilled with different pulse parameters into stainless steel. The diameter of the holes increases with both, the pulse duration and the amplitude (Tool: cylindrical Pt wire with 50 µm diameter; 3 M HCl/6 M HF; $\Phi_{wp} = -120\,mV_{Pd/H}$, $\Phi_{tool} = 80\,mV_{Pd/H}$).

strated in Fig. 6, which shows an array of holes machined into a stainless steel sheet by a cylindrical 50 µm diameter tool with different pulse amplitudes and durations. Comparison of the holes at constant pulse durations clearly shows that upon increasing the pulse duration also the hole diameter increases, *i.e.*, the spatial resolution decreases. This is conceivable considering that upon increasing the pulse amplitude, the distance between the electrodes where the

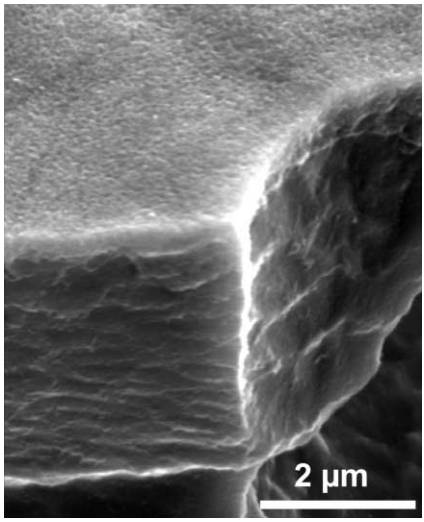

Fig. 7. Detail of a stainless steel structure, etched with 5 ns/1.8 V pulses. The surface roughness is well below 200 nm. Radii of curvature below 0.5 µm were obtained (Tool: bent W wire with 3 µm diameter; 3 M HCl/6 M HF; $\Phi_{wp} = -150\ mV_{Pd/H}$, $\Phi_{tool} = -100\ mV_{Pd/H}$).

same polarization or machining rate as previously is reached, is also increasing. Quantitative evaluation of this experiment yielded a machining precision, *i.e.*, gap width between the tool and the rime of the hole, of, for example, 5 µm for 1.5 V and 15 µm for 4 V pulses at 50 ns pulse duration.

In conclusion, the careful adjustment of pulse amplitude and pulse duration allows for machining precision in the submicrometer range, although the passivation behavior of stainless steel necessitates the use of concentrated electrolytes. Fig. 7 demonstrates the high machining precision at the detail of a structure machined with 5 ns pulse duration and 1.8 V pulse amplitude. The surface exhibits a roughness well below 200 nm and the radius of curvature at the edges reaches values below 500 nm. In principle further reduction of the pulse duration is expected to lead to further improvement of the machining precision. Considering the high electrolyte concentrations employed for stainless steel, the ion concentration in the small gap between the electrodes allows for charging of the double layer down to gap widths even below 10 nm [27]. With pulses in the 100 ps range, such machining resolutions seem to be within reach.

5. Summary and perspective

Proper choice of the electrolyte and careful adjustment of electrochemical and machining parameters allow for the machining of stainless steel with un-

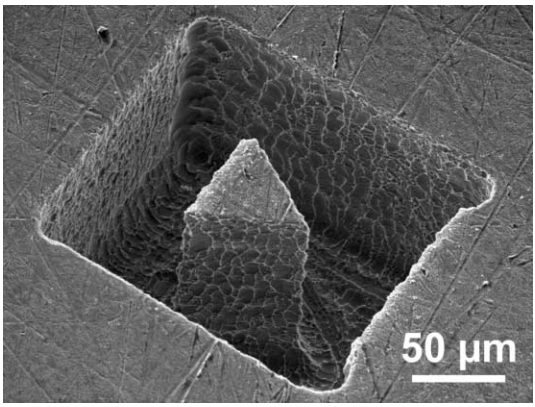

Fig. 8. A prism, designed with a computer aided design (CAD) program was automatically etched into a stainless steel sheet. A fast rough cut with 143 ns pulses was followed by a slow fine cut with 50 ns pulse duration (Tool: cylindrical W wire with 30 µm diameter; 3 M HCl/6 M HF; $\Phi_{wp} = -370\,mV_{Pd/H}$, $\Phi_{tool} = -200\,mV_{Pd/H}$).

precedented precision. The method works reliably and reproducibly, which is the prerequisite to etch complex structures and to automate the machining process. This was successfully achieved for the prism in Fig. 8. The 200 µm deep structure was machined with procedures similar to conventional milling. After the design of the structure with a commercial computer aided design (CAD) program, the path for the feed of the tool, a thin tungsten wire, was calculated. Afterwards the structure was etched in two steps: the 'rough cut' was performed with 143 ns pulses and was followed by 'fine etching' with 50 ns pulses. Contacts between tool and workpiece were in-situ monitored and the feed of the tool was correspondingly adjusted to avoid such events. The machining speed is given by the electrochemical dissolution rate of the stainless steel and by the mass transport in the gap between tool and workpiece. Therefore, the path and the movement of the tool during etching the workpiece are of crucial importance to achieve high machining speeds. To meet these challenges questions comprehensive and promising basic investigations on a suited automated microproduction technology based on electrochemical micromachining by ultrashort voltage pulses are currently performed at the IZFM.

Acknowledgement

The authors want to thank K. Weil and P. Allongue for fruitful discussions and comments. Technical support by G. Heyne and the members of the electronics laboratory of the FHI is gratefully acknowledged.

References

1. I. Amato, Science **284** (1998) 402.
2. H. G. Craighead, Science **290** (2000) 1532.
3. W. Ehrfeld, V. Hessel, and H. Löwe, *Microreactors – New Technology for Modern Chemistry*, Wiley-VCH, Weinheim (2000).
4. A. N. Cleland and M. L. Roukes, Nature **392** (1998) 160.
5. S. Kawata, H.-B. Sun, T. Tanaka, and K. Takada, Nature **412** (2001) 697.
6. K. Dunkel *et al.*, J. Micromech. Microeng. **8** (1998) 301.
7. W. Eberhardt *et al.*, in *Transducers 01*. The 11th International Conference on Solid-State Sensors and Actuators, Munich (2001).
8. *Handbook of Microlithography, Micromachining, and Microfabrication.* P. Rai-Choudhury, Ed. (SPIE Optical Engineering Press, Bellingham, WA, 1997), Vol. 1 and 2.
9. C. R. Friedrich, *et al.*, in *Handbook of Microlithography, Micromachining, & Microfabrication*. P. Rai-Choudhury, Ed., SPIE, Bellingham, WA (1997), Vol. 2, pp. 299–377.
10. M. Datta and D. Harris, Electrochim. Acta **42** (1997) 3007.
11. M. Datta and D. Landolt, Electrochim. Acta **45** (2000) 2535.
12. D. M. Kolb, R. Ullmann, and T. Will, Science **275** (1997) 1097.
13. G. E. Engelmann, J. C. Ziegler, and D. M. Kolb, Surface Sci. **401** (1998) L420.
14. W. Schindler, D. Hofmann, and J. Kirschner, J. Electrochem. Soc. **148** (2001) C124.
15. W. Li, J. A. Virtanen, and R. M. Penner, Appl. Phys. Lett. **60** (1992) 1181.
16. S. Gorer *et al.*, Electrochim. Acta **43** (1999) 2799.
17. R. Schuster, V. Kirchner, X. H. Xia, A. M. Bittner, and G. Ertl, Phys. Rev. Lett. **80** (1998) 5599.
18. X. H. Xia, R. Schuster, V. Kirchner, and G. Ertl, J. Electroanal. Chem. **461** (1999) 102.
19. M. P. Zach, K. H. Ng, and R. M. Penner, Science **290** (2000) 2120.
20. C. Madore, O. Piotrowski, and D. Landolt, J. Electrochem. Soc. **146** (1990) 2526.
21. E. Rosset, M. Datta, and D. Landolt, J. Appl. Electrochem. **20** (1990) 69.
22. E. Uhlmann, U. Doll, R. Förster, R. Nase, and R. Schikofsky, Maschinenmarkt **45** (2000) 34.
23. A. Uhlir, Rev. Sci. Instrum. **26** (1955) 965.
24. A. J. Bard and M. V. Mirkin, Eds., *Scanning Electrochemical Microscopy*, Marcel Dekker, Inc., New York (2001).
25. A. J. Bard, G. Denault, C. Lee, D. Mandler, and D. O. Wipf, Acc. Chem. Res. **23** (1990) 357.
26. D. M. Mandler and A. J. Bard, J. Electrochem. Soc. **137** (1990) 1079.
27. R. Schuster, V. Kirchner, P. Allongue, and G. Ertl, Science **289** (2000) 98.
28. V. Kirchner, L. Cagnon, R. Schuster, and G. Ertl, Appl. Phys. Lett. **79** (2001) 1721.
29. A. J. Melmed, J. Vac. Sci. Technol. B **9** (1991) 601.
30. V. Kirchner, Ph.D. thesis, Freie Universität Berlin (2001).
31. H. Kaesche, *Metallic Corrosion Principles of Physical Chemistry and Current Problems*, National Association of Corrosion Engineers (1985).
32. H. H. Strehblow, Werkst. Korros. **35** (1984) 437.
33. J. A. McGeough, *Principles of Electrochemical Machining*, Chapman and Hall, London (1974).